

See discussions, stats, and author profiles for this publication at:  
<https://www.researchgate.net/publication/30421898>

# Spectroscopic studies of structurally similar DNA-binding Ruthenium (II) complexes containing the dipyridophenazine ligand

ARTICLE *in* JOURNAL OF MOLECULAR STRUCTURE · OCTOBER 2001

Impact Factor: 1.6 · DOI: 10.1016/S0022-2860(01)00800-6 · Source: OAI

CITATIONS

38

READS

16

6 AUTHORS, INCLUDING:



**Colin G Coates**

Andor Technology

45 PUBLICATIONS 990 CITATIONS

SEE PROFILE



**John M Kelly**

Trinity College Dublin

209 PUBLICATIONS 6,471 CITATIONS

SEE PROFILE



**Andrée Kirsch - De Mesmaeker**

Université Libre de Bruxelles

142 PUBLICATIONS 3,573 CITATIONS

SEE PROFILE

# Spectroscopic studies of structurally similar DNA-binding Ruthenium (II) complexes containing the dipyrldiphenazine ligand

Colin G. Coates<sup>a</sup>, Phillip Callaghan<sup>a</sup>, John J. McGarvey<sup>a,\*</sup>, John M. Kelly<sup>b</sup>,  
Luc Jacquet<sup>b</sup>, A. Kirsch-De Mesmaeker<sup>c</sup>

<sup>a</sup>*School of Chemistry, The Queen's University of Belfast, Belfast BT9 5AG, Northern Ireland, Ireland*

<sup>b</sup>*Department of Chemistry, Trinity College, Dublin 2, Ireland*

<sup>c</sup>*Chimie Organique Physique, Université Libre de Bruxelles, 1050 Bruxelles, Belgium*

Received 20 November 2000; accepted 28 March 2001

## Abstract

Nanosecond transient resonance Raman and picosecond transient absorption spectroscopic investigations of the two structurally analogous Ru-polypyridyl complexes,  $[\text{Ru}(\text{phen})_2\text{dppz}]^{2+}$  (**1**) and  $[\text{Ru}(\text{tap})_2\text{dppz}]^{2+}$  (**2**), are presented (phen = 1,10-phenanthroline, dppz = dipyrldo [3,2-*a*:2',3'-*c*] phenazine; tap = 1,4,5,8 tetraazaphenanthrene). The findings offer insight into the differing nature of the lowest excited states of the two complexes, and describe the role of these states within the very distinct photophysical behaviour of each, both in relation to solvent response and their interaction with DNA (facilitated in each case through the intercalating dppz ligand). The active, solvent-sensitive, dppz-based <sup>3</sup>MLCT states involved in the 'light-switch' behaviour of (**1**) are probed, alongside evidence of a progression through a precursor transient state when the complex is in non-aqueous environment. Evidence has been provided of a photophysical pathway for (**2**), involving formation of a tap-based lowest <sup>3</sup>MLCT state. When (**2**) is bound to DNA through the dppz ligand, a photo-driven electron transfer process ensues between the guanine base of DNA and the lowest <sup>3</sup>MLCT state. © 2001 Elsevier Science B.V. All rights reserved.

**Keywords:** Ruthenium complex; Dipyrldiphenazine ligand; DNA; Electron transfer; Intercalation; Light-switch states

## 1. Introduction

Metal complexes, which bind to DNA, have been studied extensively by a number of research groups over recent years, with emphasis on understanding the photophysical and redox perturbations that are imposed through interaction with the DNA strand [1]. The implications for clinical/diagnostic utility and for enhancing the understanding of natural

DNA-mediated biological mechanisms are considerable.

There has been a particular interest in the 'light switch effect' exhibited by the complex  $[\text{Ru}(\text{L})_2\text{dppz}]^{2+}$  (L = 1,10-phenanthroline (phen), 2,2'-bipyridine (bpy); dppz = dipyrldo [3,2-*a*:2',3'-*c*] phenazine) in which the characteristically weak emission from the metal-to-ligand charge-transfer (MLCT) excited state in aqueous solution is greatly enhanced upon interaction with double-stranded (ds) nucleic acids [2,3]. The complex is proposed to intercalate to DNA through the dppz ligand, the extended, planar, aromatic skeleton of the ligand inserting between the stacked bases of the nucleic acid,

\* Corresponding author. Tel.: +44-2890-335450; fax: +44-2890-382117.

E-mail address: j.mcgarvey@qub.ac.uk (J.J. McGarvey).

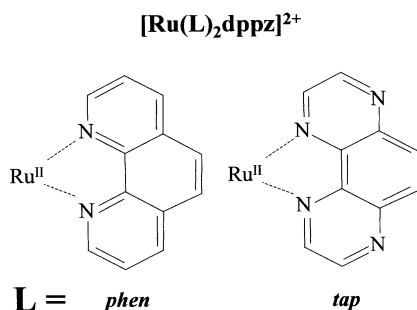


Fig. 1. Complexes with phen and tap ligands.

providing some protection to the otherwise exposed non-coordinating ‘phenazine’ nitrogens [4].

A photophysical mechanism for the effect has previously been proposed by Barbara et al. [5], derived from an investigation by single channel picosecond time-resolved luminescence and transient absorption techniques. The model involves interaction between two lowest  $^3\text{MLCT}$  states —  $\text{MLCT}^1$  and  $\text{MLCT}^2$  — the relative energies of which are sensitive to the polarity of the solvent environment, and which differ somewhat in the rate of solvent-dependent radiationless decay. A recent investigation by ourselves [6,7] using picosecond time-resolved resonance Raman ( $\text{TR}^3$ ) spectroscopy to probe  $[\text{Ru}(\text{phen})_2\text{dppz}]^{2+}$  (**1**) (structure represented in Fig. 1), has provided convincing characterisation of the light switch states involved, in good general agreement with that put forward in the Barbara mechanism. In water, using Raman signature bands for the charge transfer states involved, at each pump and probe wavelength combination employed, it was evident that decay following excitation progresses rapidly ( $\sim 5$  ps) through  $\text{MLCT}^1$  to  $\text{MLCT}^2$  from which a largely non-radiative, rapid (250 ps) decay to ground state ensues. In a less polar solvent, such as acetonitrile, Raman appears to confirm that the  $\text{MLCT}^2$  state lies inaccessibly higher in energy than  $\text{MLCT}^1$ , thus a strongly luminescent, long lived ( $>500$  ns) decay from the  $\text{MLCT}^1$  state is enabled. Interestingly, picosecond  $\text{TR}^3$  studies also appeared to point towards the existence of a ‘precursor excited state’ through which the excited complex progresses, prior to arriving at the  $\text{MLCT}^1$  state, detectable only for the complex in non-aqueous environment. It seems, from spectroscopic

characterisation of the species, that the precursor state is less likely to be charge transfer in nature. We present here further time-resolved spectroscopic investigation into the photophysical nature of (**1**), utilising picosecond transient absorption (ps-TA) involving multichannel detection in contrast to the earlier single-channel studies [5]. This work is complemented by nanosecond transient resonance Raman ( $\text{TR}^2$ ) studies.

A close structural analogue of (**1**) is the complex  $[\text{Ru}(\text{tap})_2\text{dppz}]^{2+}$  (**2**) (tap = 1,4,5,8-tetraazaphenanthrene), with the structure represented in Fig. 1. This complex also contains the dppz ligand through which binding to DNA may be reasonably expected to persist. The tap ligand is a structural analogue of phenanthroline, with extra nitrogens at the 5- and 8-positions. Interestingly, the complex  $[\text{Ru}(\text{tap})_3]^{2+}$  upon interaction with DNA, has previously been reported to be involved in photoinduced oxidation of the guanine base [1,8] based on observed quenching of luminescence, in contrast to its structural analogue  $[\text{Ru}(\text{phen})_3]^{2+}$  which actually shows slightly enhanced luminescence upon binding to DNA. The actual manner in which this latter complex binds to nucleic acid has been a subject of considerable debate, regarding the extent to which intercalative interaction is involved [1]. We present here initial photophysical investigations of (**2**), for comparison to the light-activated properties of its structural analogue (**1**). The interaction of the lowest excited state of (**2**) with DNA will also be characterised.

## 2. Experimental section

### 2.1. Materials

$\text{RuCl}_3 \cdot x\text{H}_2\text{O}$ , acetonitrile and methanol were purchased from Aldrich Sigma. The complexes were prepared as described previously for (**1**) [2,3,9,10] and (**2**) [11]. All picosecond transient absorption and nanosecond transient resonance Raman measurements were carried out on buffered solutions (10 mM phosphate + 50 mM NaCl) which were  $\sim 0.25 \times 10^{-3} \text{ mol dm}^{-3}$  in metal complex; nanosecond excited state RR measurements were made on  $\sim 10^{-4} \text{ mol dm}^{-3}$  solutions.

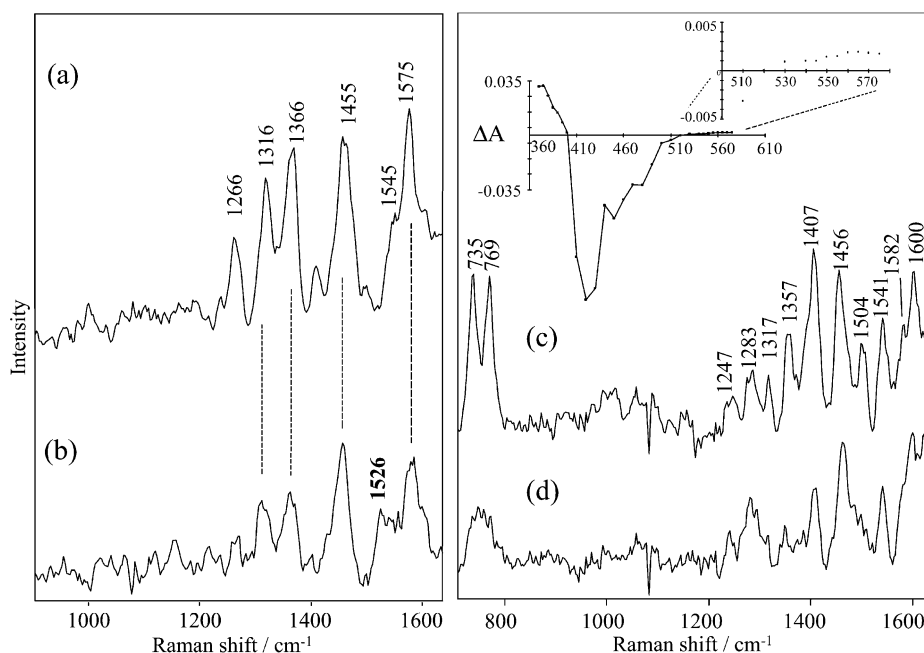


Fig. 2. Nanosecond transient resonance Raman spectra of (1) (a and b) and (2) (c and d) recorded with single colour laser pulse method (laser pulse duration ca. 8 ns) at  $\lambda_{exp} = 355$  nm: (a and c) in buffer; (b and d) [DNA phosphate]:[Ru] ratio of 20:1. Inset — point-by-point nanosecond transient absorption spectrum of (2) in buffer;  $\lambda_{exp} = 355$  nm.

## 2.2. Instrumentation

The ps-TA set-up at the Laser Support Facility, Rutherford Appleton Laboratory has been described in detail elsewhere [12–14]. Basically, a regenerative amplifier system provides a 1 ps, 800 nm pulse (0.7 mJ), which is frequency doubled to pump an optical parametric amplifier (OPA) generating a probe pulse at 0.65 kHz repetition frequencies. A ‘multifilament’ continuum is generated using 800 nm pulse,  $\sim 100$  uJ pulse energy. The continuum is dispersed using a 300 l/mm grating.

For studies in the nanosecond time range, pulsed  $\text{Nd}^{3+}$ /YAG lasers (Spectra-Physics Models DCR and GCR) were used as the excitation sources for both luminescent lifetime studies and for the transient resonance Raman ( $\text{TR}^2$ ) investigations. Kinetic traces were recorded by conventional rapid response photometry and processed using a Tektronix digitising oscilloscope (TDS 350). Nanosecond excited state resonance Raman spectra were generated by the well-known single-colour pump and probe method [15], in which the leading edge of the laser pulse

incident on the sample pumps the molecules into the excited state and the trailing edge probes the Raman scattering. Samples were contained in spinning cells in order to minimise the possibility of thermal degradation and/or photodegradation, especially where relatively long spectral accumulation times (10–15 min) at a pulse repetition rate of 10 Hz were required to obtain signals of good quality. The transient spectra were recorded with a multichannel detector (EG and G OMA III with Model 1420B intensified detector) coupled to a triple spectrometer of simple, in-house design, described earlier [15]. Incident pulse energies were typically  $\sim 3$  mJ.

## 3. Results

### 3.1. Preliminary nanosecond transient resonance Raman studies

It has been widely observed that many Ru-polypyridyl complexes yield transient absorption spectra exhibiting a strong absorption band between approx.

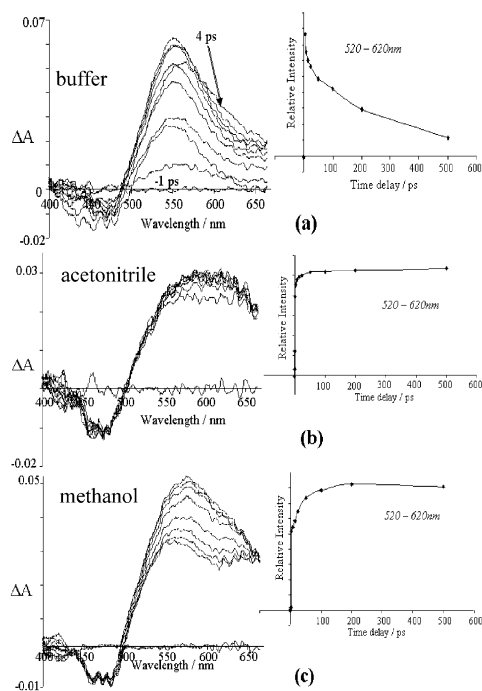


Fig. 3. Picosecond transient absorption spectra of (1): (a) in buffer, (b) in acetonitrile, (c) in methanol. Recorded by multichannel detector at a range of time delays between  $-1$  and  $500$  ps after excitation at  $\lambda_{\text{exp}} = 400$  nm (ca.  $1$  ps duration). Shown for each kinetic series is a kinetic plot derived through integration of signal intensities at pixel values between  $520$ – $620$  nm for each trace within the series.

$300$ – $400$  nm, and frequently a less intense absorption region beyond  $500$  nm [15,17]. This type of profile has indeed been reported [15,16] for (1), recorded in non-aqueous solvent environment with nanosecond flash photolysis equipment. However, it is undetectable in an aqueous environment using nanosecond time-resolution apparatus, owing to the sub-nanosecond lifetime of the lowest  $^3\text{MLCT}$  state [5,15]. In contrast however, strong luminescence ( $\lambda_{\text{max}} \sim 640$  nm) and transient absorption signals are observed for the structural analogue (2) in both aqueous and non-aqueous solvent environments, yielding exponential decays in water of  $\tau \sim 400$  ns. A point-by-point  $\Delta A$  spectrum recorded of (2) is shown in Fig. 2 inset, exhibiting a profile similar to that observed [15,16] for (1).

Fig. 2 shows single-colour nanosecond  $\text{TR}^2$  spectra recorded of (1) and (2) in the absence and presence of DNA at an excitation wavelength of  $354.7$  nm. Laser

energy and focus were such that the buffer only spectra shown represent extensive pumping to the excited state in each case. As has been previously reported [15,18], the nanosecond RR technique readily gives a spectrum of the sub-nanosecond  $^3\text{MLCT}$  excited state of (1), through generation of a pseudo steady-state population of the species within the duration of the  $\sim 8$  ns pump/probe pulse. Comparison of the spectra (a) and (c) indicate that distinct excited state species are formed within the laser pulse for each complex. The spectrum of (1) comprises several strong  $\text{dppz}^{\cdot-}$  features, e.g. at  $1266$ ,  $1316$ ,  $1366$  and  $1575$   $\text{cm}^{-1}$ , and some bands of neutral phenanthroline, indicating the formation of a lowest  $^3\text{MLCT}$  state, represented formally [19] as  $[\text{Ru}^{\text{III}}(\text{phen})_2(\text{dppz}^{\cdot-})]^{2+}$ . In contrast, the spectrum of (2) does not exhibit any bands characteristic of the  $\text{dppz}^{\cdot-}$  anion. Comparison with ground and excited state RR spectra recorded of the homoleptic complex  $[\text{Ru}^{\text{III}}(\text{tap})_3]^{2+}$  [20] indicate that the spectrum consists largely of bands attributable to the tap ligand. In this case, it appears that the vibrational features of the reduced form of tap actually exhibit only very small shifts from their respective ground state positions. Features assignable to neutral  $\text{dppz}$  ligand also contribute to the spectra. Thus, the observed spectrum can be interpreted as arising from a tap-based lowest  $^3\text{MLCT}$  state, represented as  $[\text{Ru}^{\text{III}}(\text{tap}^{\cdot-})(\text{tap})(\text{dppz})]^{2+}$ .

The effect on the  $354.7$  nm RR spectra of adding DNA to the aqueous solution of (1), shown in Fig. 2(b), has been previously described [15], resulting in both depletion of bands of the  $\text{dppz}^{\cdot-}$  anion, with respect to neighbouring neutral phen modes, and appearance of a  $\text{dppz}^{\cdot-}$  band at  $1526$   $\text{cm}^{-1}$ . Distinct effects also appear in the spectrum of (2) upon addition of DNA. In this case, however, through comparison with a series of power-resolved studies performed on the complex in *buffer only* [20], it is clear that the spectrum recorded in the presence of DNA exhibits a greater contribution from the ground state species at this probe wavelength.

### 3.2. Picosecond transient absorption studies

#### 3.2.1. $[\text{Ru}(\text{phen})_2\text{dppz}]^{2+}$ in aqueous and non-aqueous media

Fig. 3(a) shows ps-TA spectra recorded of the

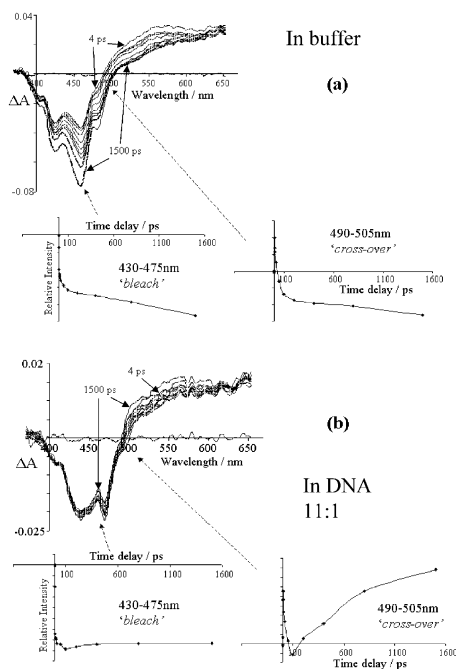


Fig. 4. Picosecond transient absorption spectra of (2): (a) in buffer, (b) [DNA phosphate]:[Ru] ratio of 11:1. Recorded by multichannel detector at a range of time delays between  $-1$  and  $1500$  ps after excitation at  $\lambda_{exp} = 400$  nm (ca.  $1$  ps duration). Shown for each kinetic series is a kinetic plot derived through integration of signal intensities at pixel values between  $430$ – $475$  nm and  $490$ – $505$  nm for each trace within the series.

complex in aqueous environment, approximately spanning the wavelength range  $400$ – $700$  nm (unfortunately, the laser-generated continuum [12,13] used as the probe has a cut-off wavelength below  $400$  nm enabling only the region of positive excited state absorption beyond  $500$  nm to be probed), the wavelength region between  $400$  and  $500$  nm being dominated largely by ground state bleach. It is evident that the long wavelength absorption maximises near  $575$  nm and falls off significantly towards the low energy edge of the spectral window. Importantly however, the transient differential absorbance ( $\Delta A$ ) traces recorded at very early time delay (ca  $4$  ps) exhibit a positive contribution to the differential absorption signal towards the lowest energy edge, more so than for later times. Fig. 3(a) also shows a kinetic plot derived by integrating the intensity across a selected wavelength range, and plotting against

time-delay. This was performed for the wavelength range  $520$ – $620$  nm and clearly shows decay of the dominant state populated in aqueous solution, over the time range covered,  $4$ – $500$  ps.

Significantly, the ps-TA spectra recorded for (1) in acetonitrile, shown in Fig. 3(b), exhibit an excited state absorption profile, which extends much further to the red than that observed in aqueous environment, suggesting the involvement of a different excited state. A kinetic plot derived from the region of long wavelength absorption indicates a non-instantaneous rise-time, suggesting transition through a state prior to the  $^3\text{MLCT}$  state, this 'precursor' state itself being non- or weakly absorbing within the wavelength range monitored.

The ps-TA measurements recorded for (1) in methanol are shown in Fig. 3(c), exhibiting behaviour comparable to that seen for the complex in acetonitrile. In this case, however, it appears from the kinetic profile shown (inset) that the absorption band of the dominant state grows in over a slightly longer time-scale than that observed in acetonitrile. It should be pointed out here that the bleach region, whilst occurring at the expected position relative to ground state absorption, appears to be of markedly lower amplitude than expected, compared to the amplitude of the positive TA region. This suggests some caution should be exercised regarding detailed interpretation of the region below  $500$  nm.

### 3.2.2. $[\text{Ru}(\text{tap})_2\text{dppz}]^{2+}$ in presence and absence of DNA

Fig. 4(a) shows ps-TA spectra recorded of (2) in buffer, over a range of time-delays between  $-1$  and  $1500$  ps. As for the ps-TA spectra of (1) (Fig. 3), the wavelength range covered was sufficient to encompass both the regions of ground state depletion between  $\sim 400$  and  $500$  nm and of positive transient absorption beyond  $500$  nm. We direct attention mainly to the latter, in view of the above remarks about artefacts in the bleach region. Indeed the kinetic plots shown in Fig. 4(a), derived from measurements in the bleach and 'crossover' region, would suggest that, rather unexpectedly, the maximum extent of bleach is attained relatively slowly. However a corresponding kinetic plot (not shown) from measurements further to the red in the positive  $\Delta A$  region shows a more expected pattern of rapid decay ( $<100$  ps) to a

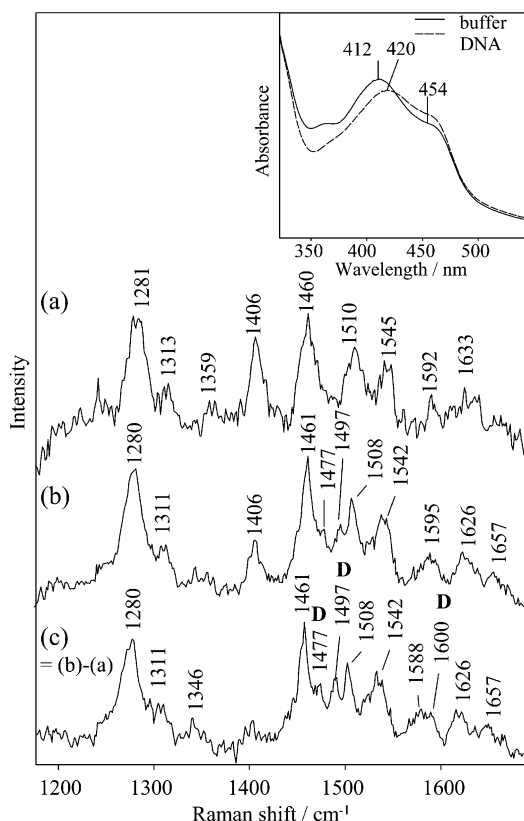


Fig. 5. Nanosecond transient resonance Raman spectra of (2): (a) in buffer, (b) [DNA phosphate]:[Ru] ratio of 20:1, recorded with single colour laser pulse method (laser pulse duration ca. 8 ns) at  $\lambda_{exp} = 400$  nm. (c) is a subtraction (b-a), scaled for complete removal of the tap<sup>+</sup> feature at  $1406\text{ cm}^{-1}$ . Inset — UV-vis absorption spectra of (2) in buffer and bound to DNA.

flat baseline). The positive  $\Delta A$  profile is typical of that for <sup>3</sup>MLCT states of Ru-polypyridyl complexes.

Fig. 4(b) shows ps-TA spectra recorded of (2) in DNA at a [DNA phosphate]:[Ru] binding ratio of 11:1. Clearly, the kinetics are significantly perturbed upon DNA binding, observable through comparison of the integrated kinetic plots shown for the ‘bleach’ and ‘zero-absorbance’ regions with the respective plots for the complex in the absence of DNA (Fig. 4(a)). As already indicated earlier for the latter, the possible intrusion of artefacts in the bleach region urges caution. Nevertheless, comparison with the plots in the presence of DNA remains of interest. The main region of positive absorption does not follow precisely the same pattern as for the complex

in the absence of DNA, the longest time delay spectrum with DNA appearing to absorb more strongly than for the isolated complex.

### 3.3. Transient resonance Raman studies at 480 nm

Fig. 5 shows transient RR spectra of (2), recorded at an excitation wavelength of 480 nm, in the presence and absence of DNA (20:1 ratio). This wavelength, acting as pump and probe in the TR<sup>2</sup> experiment, was chosen in order to probe the significant changes, which seemed to occur to the transient absorption spectra upon introduction of DNA. Shown in Fig. 5 (inset) is the ground state UV-vis spectrum of (2) under the same conditions, indicating perturbation of the higher energy MLCT absorption region upon binding of the complex to DNA.

The TR<sup>2</sup> spectrum of the complex in buffer solution (Fig. 5(a)) reveals features characteristic of the tap ligand. Dppz ground state bands are not expected to be in resonance at this wavelength (this was confirmed in a spectrum recorded of the complex with 488 nm CW excitation). Observation of the positions of the tap bands indicates small shifts in a number of features, away from their expected ground state positions. Addition of DNA causes some minor, but significant, spectral changes. The band frequencies shift slightly to the exact positions expected for tap ground state features. It can also be seen that the signal/noise ratio has actually improved in the presence of DNA. Also evident is a marked depletion of a feature at  $1406\text{ cm}^{-1}$ . There also appears to be small bands at  $1477$  and  $1497\text{ cm}^{-1}$  which correspond to two of the most prominent features previously attributed [15] to dppz ligand vibrations, enhanced via dppz-based MLCT transition(s). In order to study the bands more effectively, any residual excited state contribution to the spectrum was removed through subtraction of the spectrum recorded in buffer (trace (b-a), Fig. 5), scaled for removal of the  $1406\text{ cm}^{-1}$  band. The two dppz features can now be observed more clearly, and in addition a third dppz ground state band [15] emerges at  $1600\text{ cm}^{-1}$ , causing a broadening of the tap feature at  $1588\text{ cm}^{-1}$ . The remainder of the bands are undoubtedly due to enhancement through tap-based MLCT transitions.

#### 4. Discussion

Clear photophysical distinctions exist between the closely related complexes **(1)** and **(2)**. Fundamentally, nanosecond luminescence and transient absorption lifetime studies revealed a marked difference in decay lifetimes from the lowest  $^3\text{MLCT}$  excited state in aqueous solution, a relatively long lived (and intense) luminescence,  $\tau \sim 400$  ns, being observed for **(2)**, whereas **(1)** has previously been recognised to exhibit negligible luminescence in aqueous environment, owing to a largely non-radiative decay from the lowest  $^3\text{MLCT}$  state in this environment (the luminescent component of decay from this state,  $^3\text{MLCT}$ , occurring with  $\tau \sim 250$  ps [5]). The point-by-point  $\Delta A$  spectrum shown (Fig. 2, inset) for **(2)** in aqueous solution, recorded 10 ns after excitation, shows a profile, which is typical of a lowest  $^3\text{MLCT}$  state of a Ru-polypyridyl complex. However, whilst the  $\Delta A$  measurements confirm the charge-transfer nature of the luminescent state, more precise characterisation of the excited state(s) is necessary to account for the photophysical differences between the complexes in this (aqueous) environment. The transient RR technique has been extensively used in this respect, owing to its ability to probe subtle changes within the electronic transitions contributing to excited state absorption bands, and to provide detailed structural information on the transients concerned.

TR<sup>2</sup> spectra recorded of each complex in aqueous environment at 355 nm excitation wavelength (Fig. 2(a) and (c)), in resonance with  $\pi^*-\pi^*$  transitions of strong absorption bands of the reduced ligand in the lowest  $^3\text{MLCT}$  state, were successful in defining the fundamental distinction between the lowest excited states of **(1)** and **(2)**, exhibiting features characteristic of a tap-based  $^3\text{MLCT}$  state in the case of **(2)**, in contrast to the dppz-based  $^3\text{MLCT}$  state of **(1)** [15,20]. Essentially, the addition of two extra nitrogens to the phenanthroline ligand has had the photo-physically-significant consequence of lowering the orbital energy of the reduced ligand relative to the reduced dppz ligand, i.e. the ‘ancillary ligand’ becomes more easily reduced in the lowest  $^3\text{MLCT}$  state. The relatively small frequency shifts observed between ‘ground state’ tap vibrations and the corresponding reduced tap<sup>−</sup> vibrations of the excited state

are not surprising, given the structural similarity between tap and phen ligands. The excited state RR spectrum of the complex  $[\text{Ru}(\text{phen})_3]^{2+}$  has been reported by other groups [21] as having vibrational frequencies close to those of the ground state, indicating little nuclear displacement between the ground and lowest  $^3\text{MLCT}$  excited state. A convenient marker for the degree of excited state formation is given by the relative intensity of the tap<sup>−</sup> band at  $1408\text{ cm}^{-1}$ , which grows insignificantly with increasing pulse energy.

Upon binding to DNA, changes are evident to the spectra of both complexes. These effects have been described previously [15] for **(1)**, the depletion of features of the dppz<sup>−</sup> anion relative to neighbouring neutral phen bands occurring as a function of perturbation of  $\pi^*-\pi^*$  transitions of dppz<sup>−</sup> through intercalation of the ligand between base pairs. The  $1526\text{ cm}^{-1}$  dppz<sup>−</sup> feature can be regarded as a signature for the light-switch effect displayed by **(1)**, as observed in our recent picosecond TR<sup>3</sup> studies [6,7].

However, at this excitation wavelength, the changes that occur to the TR<sup>2</sup> spectrum of **(2)** upon binding to DNA can be interpreted largely in terms of quenching of the excited state, relative to that of unbound complex. Thus, whereas adding DNA to **(1)** has the effect of modifying the excited state nature of the complex [5–7], binding of **(2)** to DNA can be seen to result in a degree of quenching of the excited state species. However, in both complexes the binding to DNA still occurs via the dppz ligand, apparent in the perturbation of the  $^1\text{MLCT}$  absorption bands in the ground state absorption spectrum of **(2)**, shown in Fig. 5 (inset). By analogy with proposals made for related complexes [1,8], observation of such quenching can reasonably be associated with photo-induced electron transfer from a nearby guanine (the most readily oxidised of the DNA bases) to an excited state of the complex.

##### 4.1. Picosecond transient absorption studies of **(1)**

The results of the ps-TA measurements shown in Fig. 3 provide additional insight into the photophysical pathway controlling the light-switch behaviour of **(1)**. The marked changes with environment evident in the transient state absorption profile in the region beyond 500 nm (Fig. 3) reflect the involvement of two



environment-sensitive  $^3\text{MLCT}$  states —  $\text{MLCT}^1$  and  $\text{MLCT}^2$  — proposed to be responsible for the light-switch behaviour upon binding to DNA [5]. The absorption band of (1) in non-aqueous solution (Fig. 3(b) and (c)) displays an absorption profile which apparently extends to longer wavelengths, beyond the range probed here, and is attributable to the  $\text{MLCT}^1$  state which is more dominant in this environment and also displays considerable long-lived luminescence. The absorption profile in the aqueous environment (Fig. 3(a)) maximises at ca. 575 nm and clearly does not extend to longer wavelengths to the extent observed for the non-aqueous environment. The spectra in this case are attributed to the absorption of the short-lived, largely non-radiative,  $\text{MLCT}^2$  state and the kinetic profile (Fig. 3(a)) derived from the absorption data indicates significant decay of this state over the 500 ps studied. However, the absorption band recorded at a delay between excitation and probe continuum of 4 ps in this environment displays a small but discernible shoulder on the longer wavelength side, which we ascribe to progression through the  $\text{MLCT}^1$  state prior to the appearance of  $\text{MLCT}^2$ . Thus it appears that  $\text{MLCT}^1$  is only the ‘initial’ state in aqueous environment, whereas it is evidently the predominant state in the non-aqueous environment of acetonitrile, (as well as in DNA), consistent with the single-channel transient absorption studies of Barbara et al. [5] and our ultrafast  $\text{TR}^3$  investigations [6,7]. The kinetic plots derived from the long wavelength absorption band of the complex in non-aqueous environment (Fig. 3(b)) point to a delayed grow-in of the  $\text{MLCT}^1$ , suggesting involvement of a ‘precursor’ state which does not absorb significantly in this wavelength range. Such a precursor state may also be involved in the photophysical pathway of the complex in water, but may be too short-lived to be detected with the picosecond time resolution available. In this context, a species with sub-picosecond lifetime and exhibiting a considerable degree of anisotropy has recently been reported by Zewail et al. [22] for (1) in water.

#### 4.2. Picosecond transient absorption of (2)

At first inspection, the transient absorption profile of (2) in aqueous solution (Fig. 4(a)) appears to be quite similar to that observed for (1) (Fig. 3(a)), exhi-

biting a region of ground state bleach ca. 400–500 nm and a positive  $\Delta A$  signal beyond 500 nm. However, significant time-dependent differences between the two are evident upon closer inspection, as indicated earlier. The increasing magnitude and change in profile with time of the ground state bleach after the laser flash is finished might conceivably suggest progression through an absorbing intermediate excited state. However, the possibility of artefacts in the bleach region, raised earlier for (1), must again be considered. (From comparison of the profiles of these ps TA spectra to ns TA spectra [20] of (1) and (2) it is readily evident that in both cases, the bleach region in the ps data is significantly less intense than expected, relative to the positive absorption. Nevertheless, the ps spectral profiles observed for (2) may still be usefully compared to the corresponding spectra of the complex in the presence of DNA). Parallel investigations of (2) in acetonitrile showed a very similar series of spectra, indicating little solvent dependence for the spectral changes, in contrast to the marked solvent-dependent photophysics of (1).

Compared to complex (2) alone, the corresponding effects observed over the same time range (–1 to 1500 ps) on the ps-TA spectra of (2) when bound to DNA are subtle but significant. The differences become especially evident upon comparison of the kinetic plots derived from both the regions of bleach and zero absorbance cross-over (Fig. 4(b)), with the corresponding kinetic plots for the complex in the absence of DNA (Fig. 4(a)) along with the subtle differences in the overall profiles of the positive absorption at longer time delays. The overall perturbation to the spectra in the presence of DNA can be ascribed to the grow-in of a transient absorption. The fact that the main region of positive absorption does seem to be broadly similar to that seen for the complex in absence of DNA, suggests progression to a state characterised by the same  $\pi^*-\pi^*$  transitions, most likely of the anionic  $\text{tap}^{\cdot-}$  species. A  $\text{tap}^{\cdot-}$  moiety present in the species would account for the absorption in the wavelength region beyond 500 nm. Importantly however, the enhanced absorption at the higher end of this absorption band at longer time delays is indicative of grow-in of a distinct absorbing species.

Given the evidence from the  $\text{TR}^2$  nanosecond time-scale studies (Fig. 5) that the excited state of (2) when

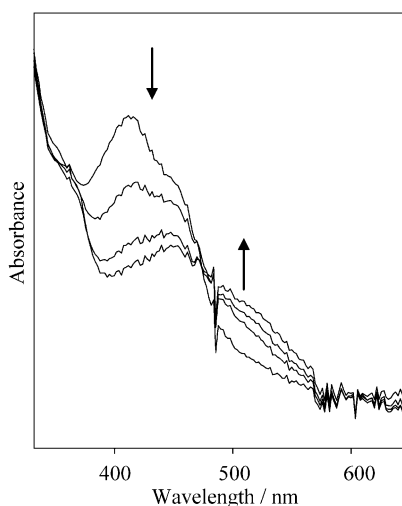
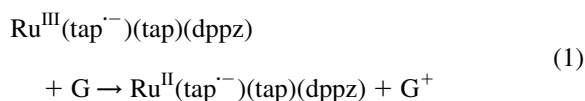


Fig. 6. Spectroelectrochemistry of first reduction of (2) in acetonitrile at  $-0.8$  V vs a standard calomel electrode on an optically transparent thin layer electrode.

bound to DNA is quenched, the most likely conclusion from the picosecond transient absorption data is that electron transfer from the DNA base, guanine, to the lowest  $^3\text{MLCT}$  state of (2) is taking place:



The  $\text{Ru}^{\text{II}}$  species resulting from such an electron transfer to the  $\text{Ru}^{\text{III}}$  centre would obviously bear considerable resemblance to the complex in its electronic ground state, with the obvious difference that one of the tap ligands would now be in anionic form. One effect of this extra electron density on a tap ligand might be to destabilise the  $d\pi$ -orbitals of the  $\text{Ru}^{\text{II}}$  centre, thus causing a red shift in the remaining MLCT transitions of the reduced complex. Given the original positions of the MLCT absorption bands of the ground state complex (shown in Fig. 5, inset), the reduced transient species may reasonably be expected to exhibit MLCT absorption in the wavelength region around or below 500 nm. What we see then in the picosecond transient absorption data for (2) bound to DNA, is this reduced species undergoing what can be described as a dynamic perturbation caused by the electron transfer from the guanine. An electrochemical ‘model’ for the guanine-reduced tran-

sient species is provided in effect by the first reduced species of (2) generated in an optically transparent thin-layer electrochemical cell. The electronic absorption spectrum of this species (Fig. 6) clearly shows depletion of MLCT absorptions and a concomitant grow-in of absorption further to the red.

Thus, a plausible photophysical picture which may now be associated with the ps-TA spectra of (2) in the absence and presence of DNA runs as follows:

1. In the absence of DNA, the  $^3\text{MLCT}$  state forms efficiently and is readily identifiable by the spectra discussed above. A similar process has been observed for the complex in acetonitrile.
2. When (2) is bound to DNA, a forward electron transfer from the guanine base to  $^3\text{MLCT}$  takes place upon formation of the latter. The electron transfer appears to occur over several hundred picoseconds, as shown by the right-hand kinetic plot in Fig. 4(b). The rate of this process is consistent with the expected dependence of the rate of electron transfer on the free energy of the reaction [23].

Further indirect evidence in support of the above photophysical picture is provided by the nanosecond  $\text{TR}^2$  spectra recorded using 480 nm as the pump and probe wavelength (Fig. 5). The fact that bands in the  $\text{TR}^2$  spectrum shift to the exact positions expected for tap ligand ground state features, accompanied by marked depletion of the feature at  $1406\text{ cm}^{-1}$ , suggests that in the presence of DNA it is mainly ground state tap features, which are being probed, due to DNA-induced quenching. The appearance of the features at  $1477$ ,  $1497$  and  $1600\text{ cm}^{-1}$ , assignable to dppz ligand vibrations enhanced via  $\text{Ru} \rightarrow \text{dppz}$  MLCT transition, is certainly consistent with a red-shifting of this transition (bringing it more into resonance with the 480 nm probe) which, as argued earlier, should accompany formation of the  $\text{Ru}^{\text{II}}(\text{tap}^{\cdot-})(\text{tap})(\text{dppz})$  species, as a result of the electron transfer process (Eq. (1)) above.

In summary, it is proposed that in the DNA-bound complex (2), three states of the complex are being probed in the  $\text{TR}^2$  spectra probed at 480 nm: (i) some residual  $^3\text{MLCT}$  excited state which has not been quenched by guanine; (ii) ground state which has been quenched, so that some tap-based features

are enhanced through the MLCT transition; (iii) a proportion of the photo-reduced species  $\text{Ru}^{\text{II}}(\text{tap}^{\cdot-})(\text{tap})(\text{dppz})$ , with dppz and tap vibrations enhanced through the respective, red-shifted MLCT transitions and  $\text{tap}^{\cdot-}$  bands enhanced via  $\pi^*-\pi^*$  intraligand transition(s) of the  $\text{tap}^{\cdot-}$  ligand. The absorption arising from the  $\pi^*-\pi^*$  transitions will most likely overlap closely with the same transition of the  $^3\text{MLCT}$  excited state, since the charge on the metal is unlikely to affect greatly such an intraligand process. Further studies are planned using ultrafast  $\text{TR}^3$  techniques to follow both forward and backward electron-transfer processes and, in the case of ps transient absorption studies, provide more definitive probing of the spectral regions marred by instrumental uncertainty.

## 5. Conclusions

Spectroscopic evidence in nanosecond and picosecond time regimes has been used to try to elucidate the nature of the lowest excited states of two closely related complexes,  $[\text{Ru}(\text{phen})_2\text{dppz}]^{2+}$  and  $[\text{Ru}(\text{tap})_2\text{dppz}]^{2+}$ , in regard to their very different patterns of photophysical behaviour, both with respect to solvent response and their interaction with DNA.

Picosecond transient absorption spectroscopy of  $[\text{Ru}(\text{phen})_2\text{dppz}]^{2+}$  has been utilised to provide evidence for the solvent-tunable light-switch states —  $\text{MLCT}^1$  and  $\text{MLCT}^2$  — in good general agreement with recent studies on the mechanism of the light switch phenomenon in the presence of DNA [5]. Evidence of a state preceding the dominant  $\text{MLCT}^1$  state in non-aqueous environment has been provided, supporting the proposal recently advanced on the basis of picosecond  $\text{TR}^3$  investigations [6,7].

Preliminary investigations on  $[\text{Ru}(\text{tap})_2\text{dppz}]^{2+}$  by the  $\text{TR}^2$  technique on a nanosecond timescale have enabled characterisation of the lowest  $^3\text{MLCT}$  excited state of the complex as being  $\text{tap}^{\cdot-}$  — localised. Significantly, the results of the studies on both pico- and nano-second timescales suggest formation of the lowest  $^3\text{MLCT}$  state of (2), to which electron transfer occurs in the presence of DNA, the forward process occurring over a timescale of several hundred picoseconds.

## Acknowledgements

We thank the UK Engineering & Physical Sciences Research Council for support of this research (Grant GR/M45696). PC thanks the Department of Education, Northern Ireland for a studentship. We wish to thank Dr Pavel Matousek and Dr Anthony Parker of Rutherford Appleton laboratories for expert assistance and guidance concerning ultrafast spectroscopic studies at the Laser Support Facility, Rutherford Appleton Laboratory.

## References

- [1] A. Kirsch-De Mesmaeker, J.-P. Lecomte, J.M. Kelly, *Top. Curr. Chem.* 26 (1996) 177.
- [2] A.E. Friedman, J.-C. Chambron, J.-P. Sauvage, N.J. Turro, J.K. Barton, *J. Am. Chem. Soc.* 4960 (1990) 112.
- [3] A.E. Friedman, C.V. Kumar, N.J. Turro, J.K. Barton, *Nucleic Acid Res.* 2595 (1991) 19.
- [4] C.G. Coates, P. Callaghan, M. Coletti, J. Hamilton, J.J. McGarvey, *J. Phys. Chem. B* 730 (2001) 105.
- [5] E.J.C. Olson, D. Hu, A. Hormann, A.M. Jonkman, M.R. Arkin, E.D.A. Stemp, J.K. Barton, P.F. Barbara, *J. Am. Chem. Soc.* 11458 (1997) 119.
- [6] Annual Report of the Central Laser Facility, 2000.
- [7] C.G. Coates, J. Olofsson, M. Coletti, J.J. McGarvey, B. Onfelt, P. Lincoln, B. Norden, E. Tuite, P. Matousek, A.W. Parker, submitted for publication, 2001.
- [8] J.-P. Lecomte, A. Kirsch-De Mesmaeker, M.M. Feeney, J.M. Kelly, *Inorg. Chem.* 6481 (1995) 34.
- [9] Y. Jenkins, A.E. Friedman, N.J. Turro, J.K. Barton, *Biochemistry* 10809 (1992) 31.
- [10] R.M. Hartshorn, J.K. Barton, *J. Am. Chem. Soc.* 5919 (1992) 114.
- [11] I. Ortmans, PhD thesis, University Libre de Bruxelles, 1997.
- [12] M. Towrie, A.W. Parker, W. Shaikh, P. Matousek, *Measurement Sci. Technol.* 816 (1998) 9.
- [13] M. Towrie, P. Matousek, A.W. Parker, S. Jackson, *Dual Diode Array System for Transient Absorption Spectroscopy*, Annual Report of the Central Laser Facility, 1998.
- [14] P. Matousek, M. Towrie, A. Stanley, A.W. Parker, *Appl. Spectrosc.* 1485 (1999) 53.
- [15] C.G. Coates, L. Jacquet, J.J. McGarvey, S.E.J. Bell, A.H.R. Al-Obaidi, J.M. Kelly, *J. Am. Chem. Soc.* 7130 (1997) 119.
- [16] J.C. Chambron, J.-P. Sauvage, E. Amouyal, P. Koffi, *Nouv. J. de Chimie* 527 (1985) 9.
- [17] J.R. Schoonover, G.F. Strouse, *Chem. Rev.* 1335 (1998) 98.
- [18] W. Chen, C. Turro, L.A. Friedman, J.K. Barton, N.J. Turro, *J. Phys. Chem. B* 6995 (1997) 101.
- [19] J.J. McGarvey, P. Callaghan, C.G. Coates, J.R. Schoonover, J.M. Kelly, L. Jacquet, K.C. Gordon, *J. Phys. Chem. B* 5941 (1998) 102.
- [20] C.G. Coates, PhD Thesis, QUB, 1996.

- [21] J.R. Schoonover, K.M. Omberg, J.A. Moss, S. Bernhard, V.J. Malueg, W.H. Woodruff, T.J. Meyer, *Inorg. Chem.* 2585 (1998) 37.
- [22] B. Oenfelt, P. Lincoln, B. Norden, J. Spencer Baskin, A.H. Zewail, *Proc. Natl. Acad. Sci. USA* 5708 (2000) 97.
- [23] G.D. Reid, D.J. Whitaker, M.A. Day, C.M. Creely, E.M. Tuite, J.M. Kelly, G.S. Beddard, *J. Am. Chem. Soc.* 6954 (2001) 123.